Journal of Contemporary Research in Chemistry (2017) 2(1): 23-34

# Structural studies of new co-crystal compound including pyridine–2,6–dicarboxilic acid and pyridine–2–carbocxamide: Synthesis and DFT calculations

Mohammad Chahkandi[1,*],Behzad Chahkandi[2]
[1]Department of Chemistry, Hakim Sabzevari University, Sabzevar, 96179-76487, Iran
Department of Chemistry, Shahrood Branch, Islamic Azad University, Shahrood, Iran

## Abstract

The proton transfer compounds (PTCs) by transferring of one or more protons from a donor group to an acceptor one are prepared .PTCs can coordinate to transition metals to form coordination complexes. In this study, colorless crystals of a new co-crystal named 2,6–pydc(py–2–cm)$_2$ through the reaction of pyridine–2,6–dicarboxilic acid (2,6–pydc) and pyridine–2–carbocxamide (py–2–cm) were prepared and characterized by FTIR, UV–Vis, and CHNS analysis. DFT calculations including geometry optimization, frequency calculations, time dependence (TD), and NBO analysis of 2,6–pydc, py–2–cm, and the proposed structure of 2,6–pydc(py–2–cm)$_2$ at B3LYP/6–311+G(d,p) level of theory using Gaussian 09 program were performed. The comparison of FTIR spectra of the synthesized 2,6–pydc(py–2–cm)$_2$ with the vibrational peaks of donor and acceptor groups confirm the inter–molecular hydrogen bond (HB) formation. The calculated UV−Vis spectrum is consistent with the experimental spectrum depicting four major electron–transition bands derived from n (p) → π* and π → π* Intra–Ligand Charge Transfer (ILCT) transitions. Moreover, the calculated stabilization energy of the prepared co-crystal that made by O−H···N O-H and N−H···O HBs measured as – 161.92 kcal mol$^{-1}$.

**Keywords:** *Co-crystal ligand; 2,6–pydc(py–2–cm)$_2$; DFT; Charge transfer; Hydrogen bonding.*

---

*Corresponding author E-mail: m.chahkandi@hsu.ac.ir (Mohammad Chahkandi)

## Introduction

From the past decade to now, chemists especially inorganic and organic experts attract to study the non–covalent interactions like hydrogen bonding (HB), van der Waals forces, π stacking, host–guest interactions, and so on made the huge compound network. There is no electron transfer but atoms and actually molecules attracted together. The weak bonds prepare remarkable binding energy to form a stable crystalline network structure. These interactions through self–assembly process build a stable network. The proton transfer compound (PTC) prepared with formation of HB and proton transfer reaction between donor and acceptor proton groups (Ganesan, et al., 2004; Smith et al., 2007; Smith et al., 2006; Smith et al., 2002; Smith et al., 2005; Yunus et al., 2017; Eshtiagh-Hosseini, et al., 2010). 2-Aminopyrimidine (2-apym), pyridine–2,6–dicarboxilic acid (2,6–pydc), and so on with multiple proton acceptor sites having the capability to participate in hydrogen bonding can be an important component for generating supramolecular structures (Chahkandi, 2016; Mirzaei, et al., 2012). Molecular functionalities, e.g. amino, hydroxyl, carboxylate, play essential roles in studying the spatial relationship between adjacent fragments resulting in repetitive van der Waals patterns or supramolecular synthons (Jeffrey, 1991). While HB has crucial roles in molecular construction, function, and dynamics of the great numbers of chemical and biological compounds (Steiner, 2002; Grabowski, 2011 and 2006) the measuring of stabilization and binding energies of non–covalent interactions in a metal organic framework (MOF) structure has not received much attention. Because of variety of structural denticity of Schiff bases as the obvious choice (Bose, 2004), selectivity and sensitivity toward transition metal ions, they picked up. In these years, computational calculations as a complement to experimental research show the usefulness to better describing the structure, stabilization energy, inter–molecular bonds vibrational frequencies, free energy surfaces, and other properties of studied complexes to designing the new better ones (Krámos, 2008; Chrappová, 2009). Not considering the dispersion energy is the main failure of Density Functional Theory (DFT) methods. Therefore, a new suggested approach is applying of a combination of DFT−D (dispersion energy corrected) with a GGA functional (like B3LYP) and a medium basis set (Riley, 2010). The dynamic properties of non–covalent interactions of small molecules can be theoretically studied in a successful reliable manner using this mentioned technique (Chahkandi, et al., 2017; Chahkandi, et al., 2016; Eshtiagh-Hosseini, et al., 2013; Mirzaei, et al., 2012). In this work, new co-crystal formulated as 2,6–pydc (Py–2–cm)$_2$ (**1**) was synthesized that pyridine–2–carbocxamide (py–2–cm) ligand having basic carboxamide group and pyridine–2,6–dicarboxilic acid (2,6–pydc) ligand having acidic carboxylate moiety play the role of proton acceptor and donor, respectively. It can be proposed that, N–H···O and O−H···N HBs construct the related network. First of all, the synthetic route and characterization of **1** proposed and in following with the aid of DFT calculations its molecular and electronic structures investigated. Finally, the respective UV spectrum studied.

## Materials and Methods

### Materials and measurements

All chemicals used in this work were analytical A.R grade. Pyridine–2,6–dicarboxilic acid (99%) and pyridine–2–carbocxamide (99%) were purchased from Merck Company and used without further purification. FTIR spectra were recorded on thermo Scientific Nicolet iS10 spectrophotometer in ATR mode (4000–400 cm$^{-1}$) in KBr discs for the free ligands and all the prepared compounds. UV–Vis spectra of aqueous solution of **1** was recorded on UV–1800 Shimadzu using UV probe version 2.32 control software for Shimadzu UV–Vis (–NIR) spectrophotometers

### Co-crystal compound synthesis

10 ml aqueous solution of 2,6–pydc (0.1 M) was added to 10 ml aqueous solution of py–2–cm (0.2 M). The mixture was stirred for 30 min in 90 °C and then the resulting colorless solution was filtered. By slow evaporation of the solvent, at room temperature, fine needle−like colorless crystals of **1** were obtained after one week. Yield: 55 % (based on Co). M.p. 180 ºC Anal. Calc. for $C_{19}H_{17}N_5O_6$ (MW: 411 gmol$^{-1}$): C, 55.47; H, 4.14; N, 17.03 %. Found: C, 55.35; H, 4.51; N, 17.01%. IR (KBr pellet, cm$^{-1}$) ν: 2870 & 2480 (O−H), 1710 $(C=O)_{\text{carboxamide}}$, 1660$(C=O)_{\text{carboxylate}}$, 1260 & 1310 (C−OH). UV−Vis: 65, 90, 133, and 280 nm.

### Computational Methods

DFT calculations have been done using B3LYP functional with the aid of Gaussian 09 (Frisch, et al., 2009) program. The structure of 2,6–pydc and py–2–cm fragments and the suggested one for **1** by Chem 3D and Gauss View softwares were built and their geometry optimization and vibrational frequencies using B3LYP/6−311+g(*d*, *p*) (Lee, et al., 1988; Becke, 1993 and 1988) level of theory were performed (The Cartesian coordinates of optimized structures have been collected in supporting information). The optimized structures are true minima in potential energy surface without any imaginary frequency (NImag = 0). Then, the electronic UV–Vis spectrum was calculated in gas phase about the optimized structure of **1** using time–dependent DFT (TD–DFT) method. Moreover, water solvent effects (ε = 78.39) on UV−Vis spectrum of **1** were followed with the polarizable continuum model (PCM) (Cances, et al., 1977). However, the both excited states of singlet and triplet were considered; while as expected the excitations to triplet ones were prohibited. Natural bond orbital (NBO) and partial atomic charges analyses of the optimized geometry of **1** were also carried out. The binding energies of the stabilizing non–covalent bonds of 2,6–pydc and py–2–cm fragments in **1** (see Fig. 1) were evaluated. Using B3LYP–D (Jurecka, et al., 2007) functional as dispersion–corrected DFT and applying the basis set superposition error (BSSE) by the mean of Boys–Bernardi counterpoise technique (Boys, et al., 1970) the calculated energies of involved interactions were corrected.

## Results and Discussion

### Optimized molecular geometric: Hydrogen bond

The optimized structure of **1** as a new synthesized co-crystal has been shown in Fig. 1. The experimental and theoretical IR spectra of **1** (depicted in Fig. 2) indicate the presence of carboxylate and carboxamide functional groups. There are stretching vibration of the O–H of carboxylate (Exp. 2480 and 2870, Calc. 2861 and 3621 cm$^{-1}$) and the intense peak that attributed to the stretching frequencies of C=O of carboxylate (Exp. 1710, Calc. 1755 cm$^{-1}$) functionality of the compound **1**. In addition, stretching vibration of C=O of carboxamide (Exp. 1660, Calc. 1743 cm$^{-1}$) were observed. Whole of FT−IR spectra peaks of synthesized and theoretical recorded spectra of similar compounds (Renuga, et al., 2014; Karakaya, et al., 2015; George, et al., 1971) and B3LYP/6-311G+(*d,p*) optimized of **1** show good consistency (cf. Table 1). Based on Fig. 1, N–H···O and O–H···N HBs constructed due to proton transfer between 2,6–pydc (proton donor) and py–2–cm (proton acceptor) groups that stabilize compound **1**. However, comparison of IR spectra of donor and acceptor groups (IR spectra omitted) with compound **1** confirms formation of the mentioned HBs. As we know, IR spectroscopy is a powerful and sensitive tool for recognition of HB formation through stretching frequency changing of D–H···A (D: donor, A: acceptor) bond. The experimental vibrational frequency of stretching mode of CO−H of carboxylate group in 2,6–pydc and **1** are 3157 cm$^{-1}$ (Calc.: 3803 cm$^{-1}$) and 2480 cm$^{-1}$ (Calc.: 2861 cm$^{-1}$), respectively. Also, symmetric stretching mode of N−H bond of carboxamide functional group in py–2–cm and **1** are 3400 cm$^{-1}$ (Calc.: 3575 cm$^{-1}$) and 3250 cm$^{-1}$ (Calc.: 3558 cm$^{-1}$), respectively. Reducing these mentioned frequencies in **1** comparing with the precursors (donor and acceptor of proton) confirms the HB formation in the synthesized co-crystal of **1**. Moreover, changing of N−H and O−H bond lengths in **1** and precursors shows the proton transferring. As is obvious in Fig. 1 lengthening of these bonds in **1** resulted in decreasing of the related vibrational frequencies and HB formation.

**Table 1** Vibrational frequencies of synthesized and B3LYP/6–311+G(*d*, *p*) optimized structures of **1**.

| **Assignments** | **Calc. for 1 (B3LYP/6–311+G(*d*, *p*))** | **Exp. for 1** | **Exp. for others** (Renuga, et al., 2014; Karakaya, et al., 2015; George, et al., 1971) |
|---|---|---|---|
| C–O–H bend. (out of plane) | 690 m | – | – |
| C–NH$_2$ bend. (out of plane) | 734vw | – | 758 |
| C−C−C (py) bend. (in plane) | 1017,1019vw | 1058 | 1032 |
| C–O–H bend. (in plane) | 1234m | 1253 | – |
| C–N str. (py) | 1291 w | – | 1296 |
| C=N str. | 1609 m | – | – |
| NH$_2$ scissoring | 1613, 1636 m | 1624 | 1647 |
| C=C & C–N str. (N–py) | 1625, 1629 m | 1632-45 | 1500–1600 |
| C=O str. (amide) | 1743, 1748vs | 1662 | 1694 |
| C=O str. (acid) | 1755, 1824 vs | 1695 | 1730–1760 |
| CO−H str. (acid) | 2861vs | 2480 | 2915 |
| C–H Ar str. | 3165-3220 vw | 3046-3300 | − |
| N–H sym. str. (amide) | 3558, 3592 m | 3250 | 3574 |
| CO−H str. (acid) | 3621 m | 3296 | 3440–3630 |
| N–H asym. str. (amide) | 3700, 3717 m | 3658-3740 | 3620−3800 |

The scrutiny of HB formation, the respective stabilization energy of them was measured. The calculated negative of stabilization energy (nfe) ($E_{nfe} = E_{network} - nE_{monomer}$) indicates that its constructed structure, stabilized via non–covalent interactions.

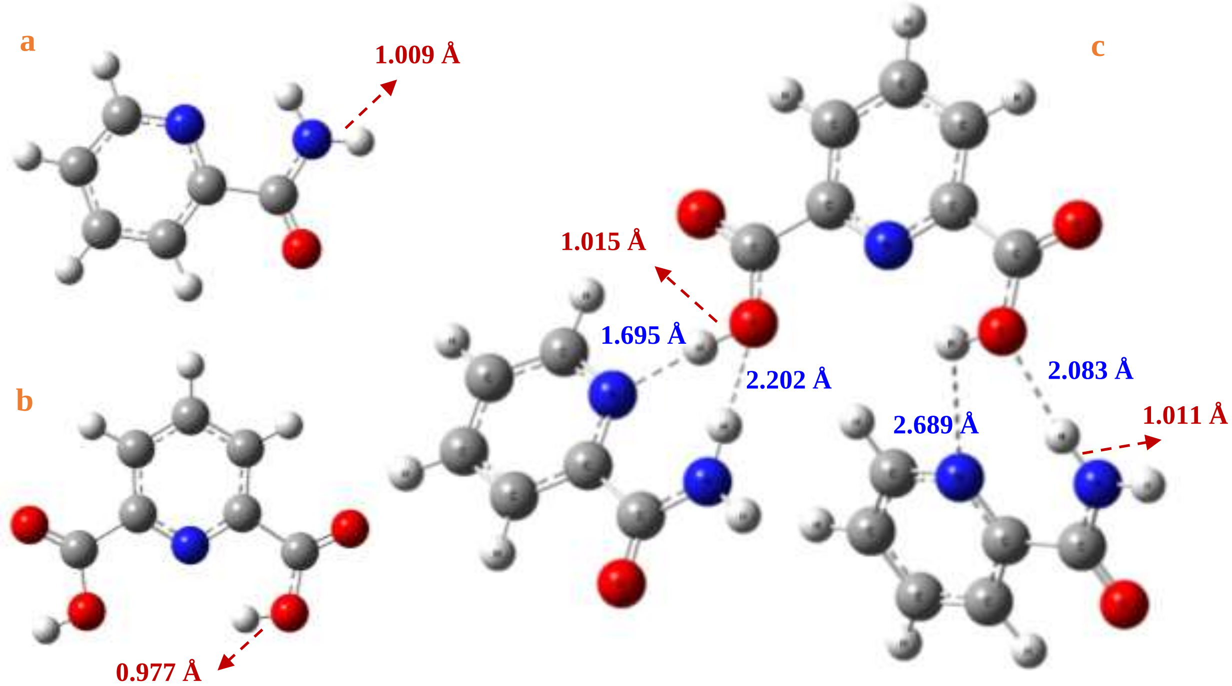

**Fig. 1** Optimized structures of (a) Py–2–cm, (b) 2, 6–pydc and c) 2,6–pydc (Py–2–cm) at B3LYP/6–311+G(*d*, *p*) level of theory. HBs shown in dashed lines in white.

In fact, two N–H···O (2.083, 2.202 Å) and two bonds of O–H···N(1.695, 2.689 Å) make the compound **1** stabilize. The total stabilization energy of **1** due to these HBs are −161.92 kcal mol$^{-1}$ that their binding energies of every mentioned HB are −38.62, −41.06, −29.21, and −53.03 kcal mol$^{-1}$. It should be noted our obtained results have good consistency with the previous reports (Seth, et al., 2011).

## Electronic spectrum

The experimental UV−Vis spectra and computed of **1** in gas and water (using PCM method) phases have been shown in Fig. 3. They look like each other and have three wide bands in ultraviolet range of 200−400 nm. The experimental spectrum (recorded about aqueous solution) shows blue shift in comparison to theoretical ones that is because of presence of water solvent molecules making HB with amide and carboxyl moiety of **1** and changes the electronic states energy. Disregarding the solvent effect on excited states of **1** and using the random–phase approximation (RPA) (Fernando, et al., 2005) in TD−DFT method caused to red shift observations. The major absorbance peaks of experimental bands observed at 65, 90, 133, and 280 nm. Two first ones having most intense can correlated to electron transitions (ETs) between solvent states and between states of solvent molecules and states of compound **1**. The calculated electronic spectrum of **1** using the TD−DFT method at B3LYP/6-311+G(*d*, *p*) level of theory shows three wide bands with maximum intensity at 174, 190, and 232 nm. However, four sharp bands at 171.90, 176.14, 186.48, and 191.25 nm for calculated spectrum in gas phase and five bands at 171.70, 177.50, 178.56, 199.17, and 231.42 nm for calculated one in water phase observed (see Figs.3 (b) and (c)). All of these should be assigned to the wide experimental band at 100−300 nm (Fig. 3 (a)). The energies and wavelengths of involved ETs and related details of the B3LYP/6-311+G(*d*, *p*)−optimized **1** are given in Table 2. Calculated spectrum in gas phase: The first calculated band at 171.70 nm is attributed to the charge transfer (CT) from 98 (HOMO−9) with n (*p*) atomic orbital character to anti−bonding 113 (LUMO+5) with π* character. The second one at 176.14 nm is correlated to CT from atomic 104 (HOMO−3) with n (*p*) character to anti−bonding 115 (LUMO+7) with π* character. Since all of the involving orbitals in these discussed bands located on acceptor group of Py–2–cm, they are assigned to n (*p*) → π* of intra−ligand charge transfer (ILCT). The third and fourth transitions calculated at 186.48 nm are correlated to CTs from 92 (HOMO−15) and 91 (HOMO−16) with π molecular orbital character to anti−bonding 109 (LUMO+1) with π* character, respectively. It should be noted that all of involving orbitals in these two bands placed on proton donor group of 2,6–pydc and attributed to π → π* of ILCT (see Fig. 4). Calculated spectrum in water phase: The first calculated band at 171.70 nm is assigned to CT from 104 (HOMO−3) with n (*p*) character located on Py–2–cm acceptor group to anti−bonding 114 (LUMO+6) with π* character located on donor group of

2,6–pydc. The second and third bands at 177.50 and 178.56 nm are related to CT from 92 (HOMO−15) with $\pi$ molecular orbital character located on 2,6–pydc and 97 (HOMO−10) with $\pi$ molecular orbital character located on Py–2–cmto anti−bonding 111 (LUMO+3) with $\pi^*$ character located on Py–2–cm. Therefore, the second and third bands are assigned to $\pi \rightarrow \pi^*$ of LLCT and ILCT, respectively. The fourth transition calculated at 199.17 nm are correlated to CTs from 94 (HOMO−13) with $\pi$ character to 108 (LUMO) with $\pi^*$ character mostly located on 2,6–pydc group. Finally, the fifth band at 231.42 nm is attributed to CT from 100 (HOMO−7) with $\pi$ character to anti−bonding 110 (LUMO+2) with $\pi^*$ character, mostly located on Py–2–cm group. It can be concluded that these two last bands are attributed to $\pi \rightarrow \pi^*$ of ILCT of 2,6–pydc and Py–2–cm, respectively (see Fig. 5). The calculated energies of frontier molecular orbitals (FMOs) have been collected in supporting information (See Table S1).

**Table 2** Experimental and calculated −B3LYP/6-311+G(*d*, *p*)electronic data in gas and water for **1**.

| Exp. Wave length (nm) | **Gas Phase** | | | |
|---|---|---|---|---|
| | Wave Length(nm) | $\Delta E_{ad}$ (ev) | Oscillator strength | Electronic transition |
| 240–300 | 191.25 | 6.483 | 0.417 | 91 (HOMO–16) → 109 (LUMO+1) |
| 120–160 | 186.48 | 6.649 | 0.340 | 92 (HOMO–15) → 109 (LUMO+1) |
| 120–160 | 176.14 | 7.039 | 0.242 | 104 (HOMO–3) → 115 (LUMO+7) |
| 80–100 | 171.90 | 7.213 | 0.330 | 98 (HOMO–9) → 113 (LUMO+5) |
| | **Water Phase** | | | |
| 240–300 | 231.42 | 5.358 | 0.125 | 100 (HOMO–7) → 110 (LUMO+2) |
| 120–160 | 199.17 | 6.225 | 0.359 | 94 (HOMO–13) → 108 (LUMO) |
| 80–100 | 178.56 | 6.944 | 0.288 | 97 (HOMO–10) → 111 (LUMO+3) |
| 80–100 | 177.50 | 6.983 | 0.306 | 92 (HOMO–15) → 111 (LUMO+3) |
| 80–100 | 171.70 | 7.223 | 0.394 | 104 (HOMO–3) → 114 (LUMO+6) |

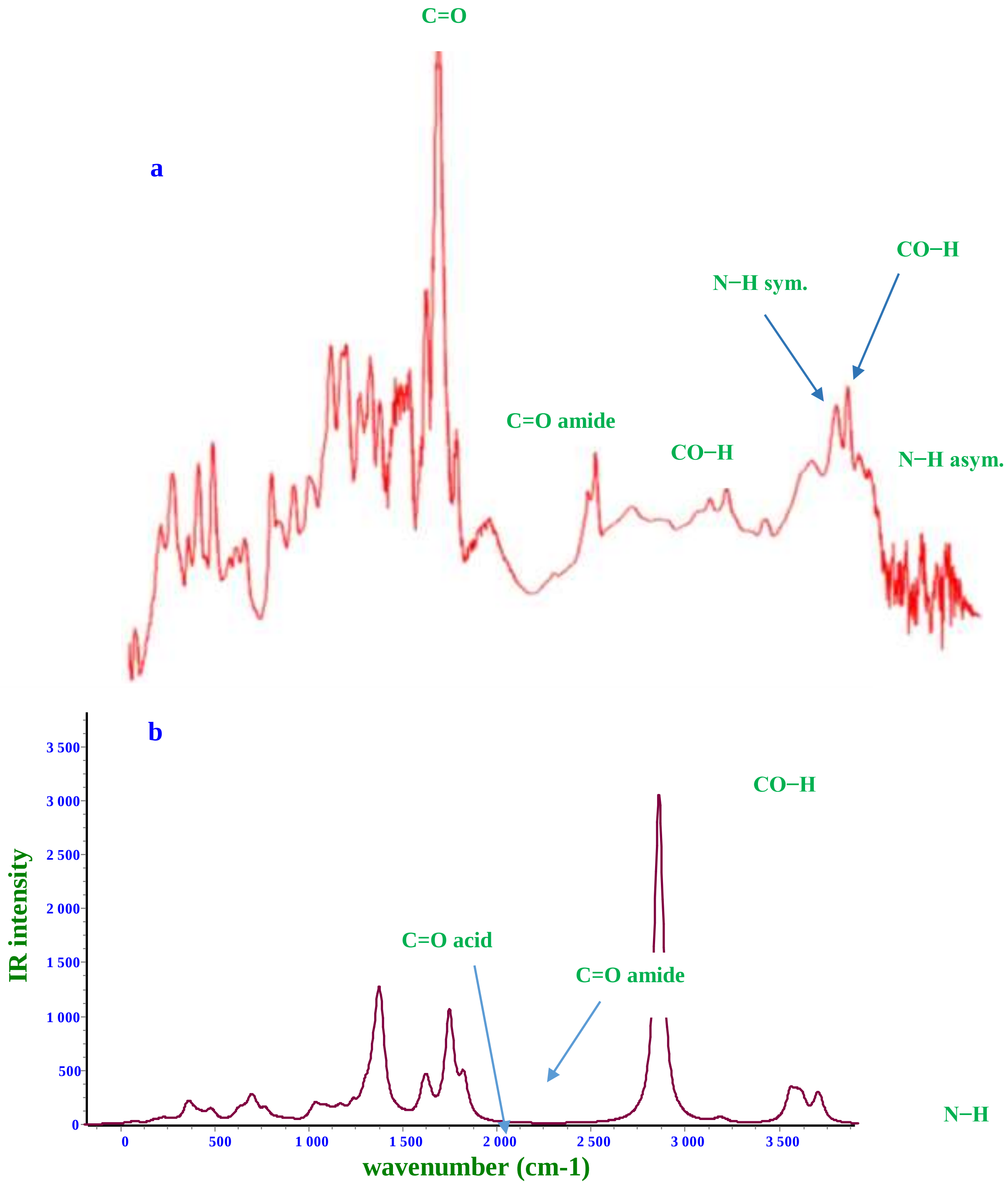

**Fig. 2** Experimental (a) and theoretical (b) FTIR ($cm^{-1}$) spectrum for **1**.

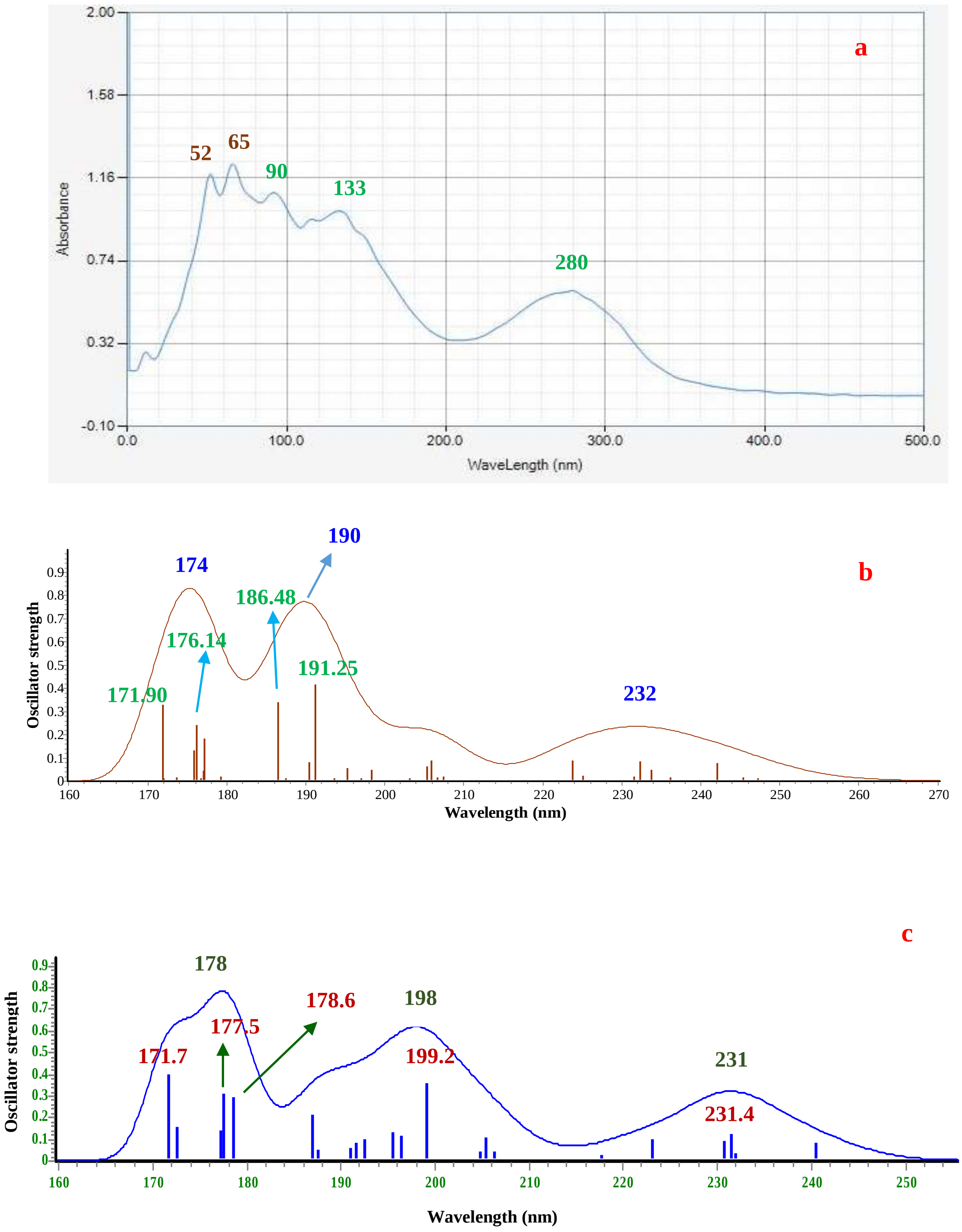

**Fig. 3** Experimental electronic spectra of **1**(a) in water, (b) calculated–B3LYP/6–311+G(*d*, *p*) in gas phase, and (c) calculated–B3LYP/6–311+G(*d*, *p*) in water solvent base on PCM method.

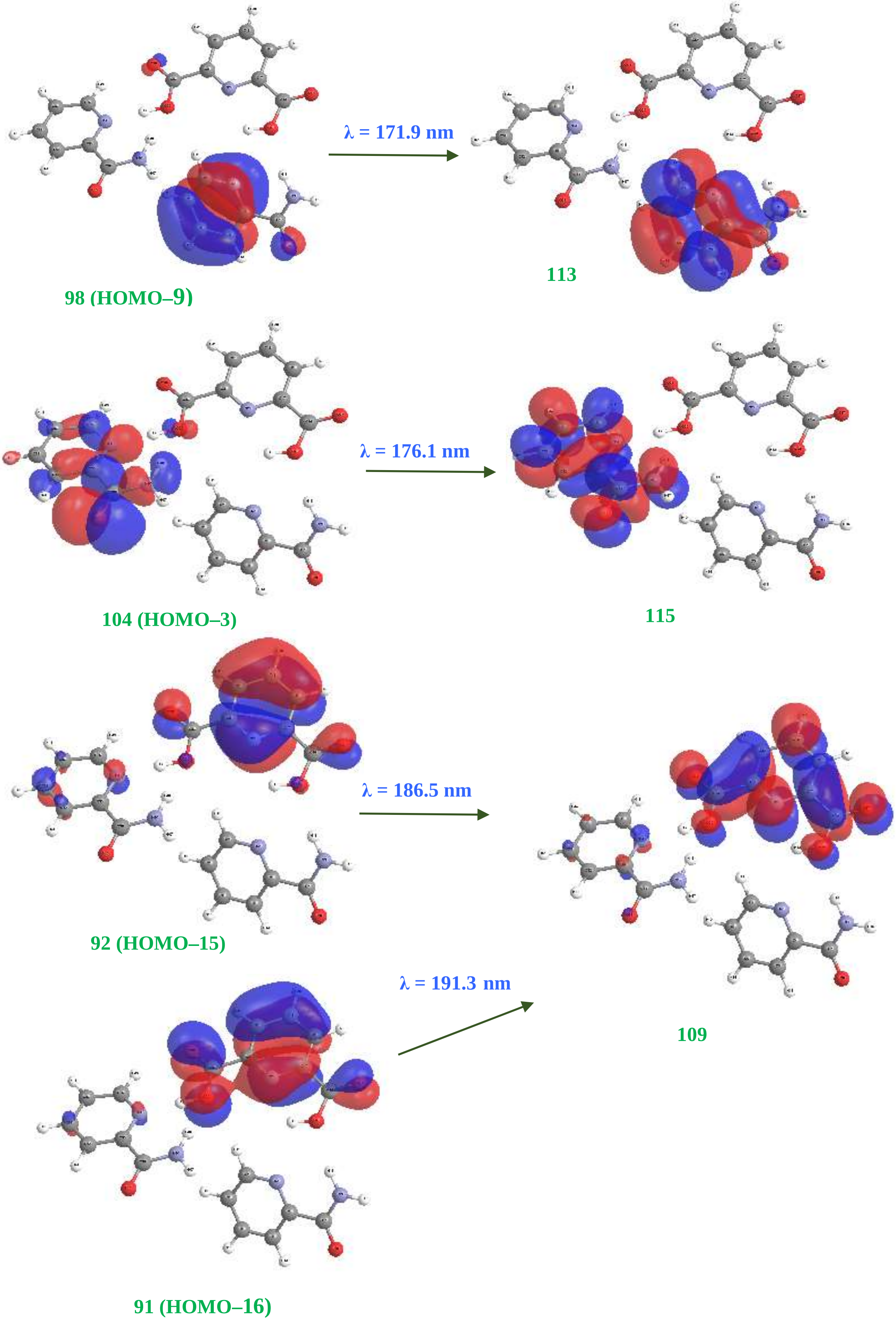

**Fig. 4** Transitions of frontier molecular orbitals for optimized–B3LYP/6–311+G(*d*, *p*) of **1** in gas phase.

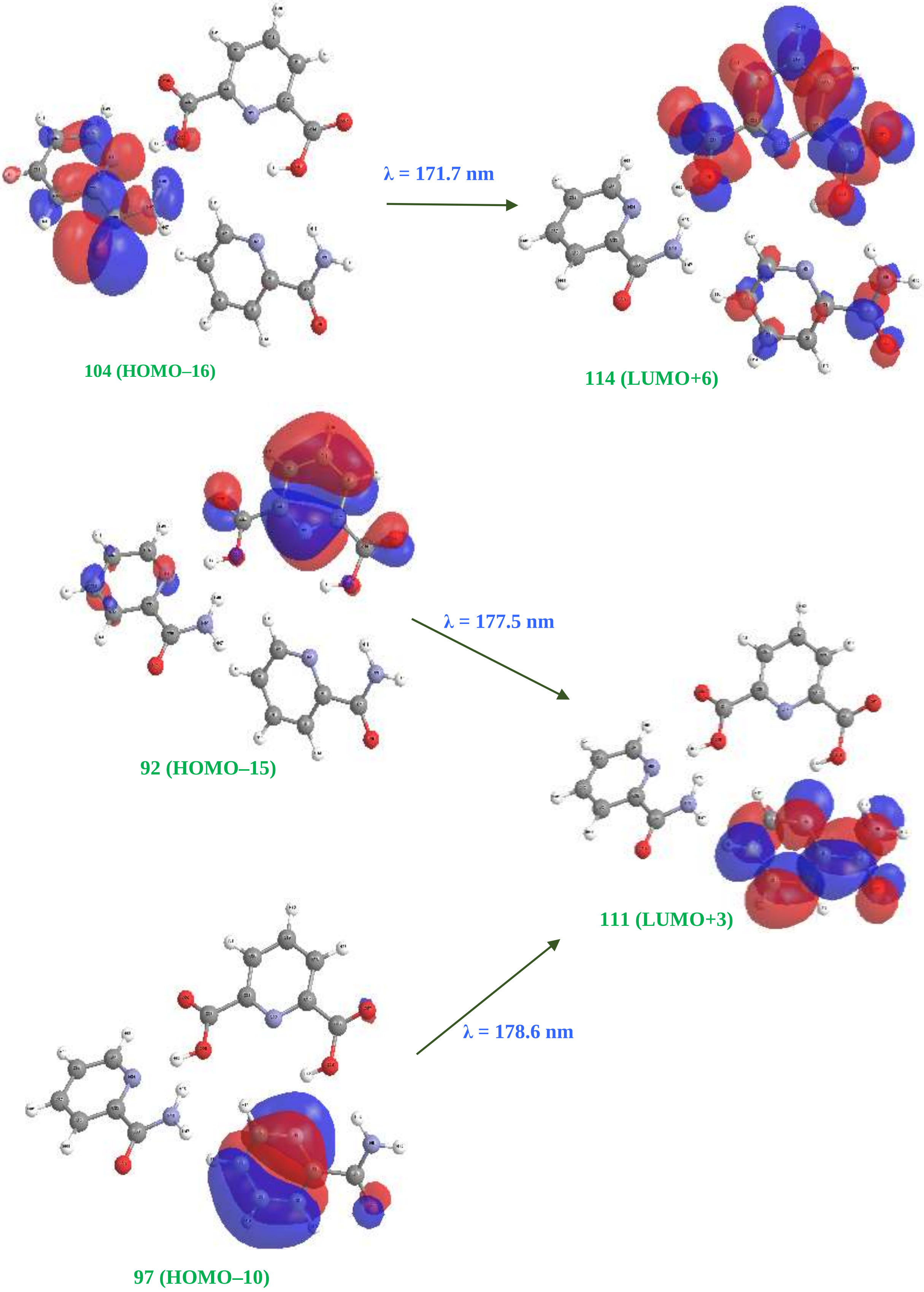
104 (HOMO–16)
λ = 171.7 nm
114 (LUMO+6)
92 (HOMO–15)
λ = 177.5 nm
111 (LUMO+3)
λ = 178.6 nm
97 (HOMO–10)

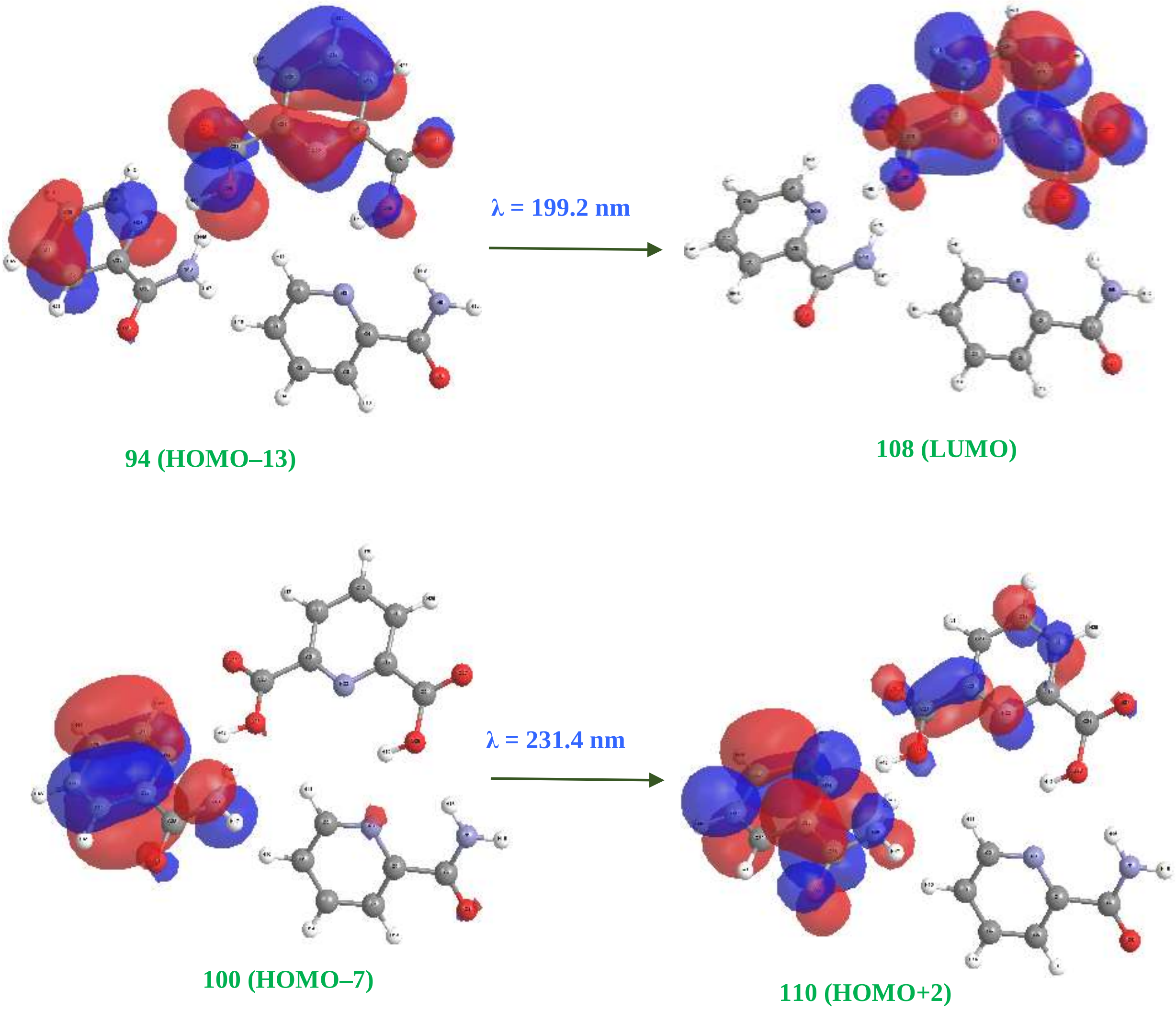

**Fig. 5** Transitions of frontier molecular orbitals for optimized–B3LYP/6–311+G(*d*, *p*) of **1** in water phase.

## Conclusions

In this research, the new synthetic co-crystal compound, with proposed formula: 2,6–pydc $(Py–2–cm)_2$ was reported and by the FTIR, UV−Vis, and CHNSO elemental analysis, characterized and studied. Comparison of vibrational frequencies of O−H and N−H bonds confirm the formation of the related HBs between proton donor and acceptor groups. The remarkable reduce of vibrational wavenumbers in **1** comparing with the precursors observed. The DFT−D calculations show N−H···O and O−H···N HBs makes **1** stabilize in amount of −161.92 kcal $mol^{-1}$. Theoretical electronic spectra in gas and solvent phases are in good agreement with the experimental spectrum but some blue shift was observed. NBO analyses suggest that the electronic bands are mainly assigned to n (*p*) $\rightarrow \pi^*$ and $\pi \rightarrow \pi^*$ of ILCT and LLCT transitions.

**Supporting Information**: Including calculated energies of FMOs and the Cartesian coordinates of optimized−B3LYP/6-311+G(*d*, *p*) of **1**.

**Author(s) contribution statement** All authors certify the candidate's stated contribution to the publication is accurate.

**Conflict of Interest** There is no conflict of interest.

**Acknowledgements** MCH gratefully acknowledges the financial support by the Hakim Sabzevari University, Sabzevar, Iran.

## References

Becke, A. D. (1993). Density-functional thermochemistry. III. The role of exact exchange. *The Journal of chemical physics*, *98*(7), 5648-5652.

Becke, A. D. (1988). Density-functional exchange-energy approximation with correct asymptotic behavior. *Physical review A*, *38*(6), 3098.

Bose, D., Banerjee, J., Rahaman, S. H., Mostafa, G., Fun, H. K., Walsh, R. D. B., ... & Ghosh, B. K. (2004). Polymeric end-to-end bibridged cadmium (II) thiocyanates containing monodentate and bidentate N-donor organic blockers: supramolecular synthons based on π–π and/or C–H··· π interactions. *Polyhedron*, *23*(12), 2045-2053.

Boys, S. F., & Bernardi, F. D. (1970). The calculation of small molecular interactions by the differences of separate total energies. Some procedures with reduced errors. *Molecular Physics*, *19*(4), 553-566.

Cances, E., Mennucci, B., & Tomasi, J. (1997). A new integral equation formalism for the polarizable continuum model: Theoretical background and applications to isotropic and anisotropic dielectrics. *The Journal of chemical physics*, *107*(8), 3032-3041.

Chahkandi, M., Bhatti, M. H., Yunus, U., Shaheen, S., Nadeem, M., & Tahir, M. N. (2017). Synthesis and comprehensive structural studies of a novel amide based carboxylic acid derivative: Non–covalent interactions. *Journal of Molecular Structure*, *1133*, 499-509.

Chahkandi, M. (2016). Theoretical investigation of non-covalent interactions and spectroscopic properties of a new mixed-ligand Co (II) complex. *Journal of Molecular Structure*, *1111*, 193-200.

Chrappová, J., Schwendt, P., Sivák, M., Repiský, M., Malkin, V. G., & Marek, J. (2009). Dinuclear fluoro-peroxovanadium (V) complexes with symmetric and asymmetric peroxo bridges: syntheses, structures and DFT studies. *Dalton Transactions*, (3), 465-473.

Mendizabal, F., & Olea-Azar, C. (2005). Theoretical study of the electronic spectrum of binuclear gold (I) complexes. *International journal of quantum chemistry*, *103*(1), 34-44.

Eshtiagh-Hosseini, H., Mahjoobizadeh, M., Mirzaei, M., Fromm, K., & Crochet, A. (2010). A new three dimensional proton transfer compound including citric acid and 2, 4, 6-triamine-1, 3, 5-triazine: synthesis, characterization and X-ray crystal structure. *European Journal of Chemistry*, *1*(3), 179-181.

Eshtiagh-Hosseini, H., Chahkandi, M., Housaindokht, M. R., & Mirzaei, M. (2013). Bromide oxidation mechanism by vanadium bromoperoxidase functional models with new tripodal amine ligands: A comprehensive theoretical calculations study. *Polyhedron*, *60*, 93-101.

Frisch, M. J. E. A., Trucks, G. W., Schlegel, H. B., Scuseria, G. E., Robb, M. A., Cheeseman, J. R., ... & Nakatsuji, H. (2009). Gaussian 09, revision a. 02, gaussian. *Inc., Wallingford, CT*, *200*.

Ganesan, S. V., & Natarajan, S. (2004). Synthesis and structures of new pyromellitate coordination polymers with piperazine as a ligand. *Inorganic chemistry*, *43*(1), 198-205.

George, W. O., Green, J. H. S., & Pailthorpe, D. (1971). The OH stretching vibrations of 2-hydroxy carboxylic acids. *Journal of Molecular Structure*, *10*, 297-299.

Grabowski, S. J. (2011). What is the covalency of hydrogen bonding?. *Chemical Reviews*, *111*(4), 2597-2625.

Grabowski, S. J. (Ed.). (2006). *Hydrogen bonding: new insights* (Vol. 3). Dordrecht: Springer.

Saenger, W., & Jeffrey, G. A. (1991). *Hydrogen bonding in biological structures*. Springer-Verlag, Berlin.

Jurečka, P., Černý, J., Hobza, P., & Salahub, D. R. (2007). Density functional theory augmented with an empirical dispersion term. Interaction energies and geometries of 80 noncovalent complexes compared with ab initio quantum mechanics calculations. *Journal of computational chemistry*, *28*(2), 555-569.

Karakaya, M., & Yildiz, M. (2015). A study on optimum transition state and tautomeric structures of a bis-heterocyclic monoazo dye. *Indian Journal of Physics*, *89*(2), 107-114.

Krámos, B., & Kovács, A. (2008). Metal–ligand interactions in Fe (II)-dioxime complexes. *Journal of Molecular Structure: THEOCHEM*, *867*(1-3), 1-4.

Lee, C., Yang, W., & Parr, R. G. (1988). Development of the Colle-Salvetti correlation-energy formula into a functional of the electron density. *Physical review B*, *37*(2), 785.

Mirzaei, M., Eshtiagh-Hosseini, H., Chahkandi, M., Alfi, N., Shokrollahi, A., Shokrollahi, N., & Janiak, A. (2012). Comprehensive studies of non-covalent interactions within four new Cu (II) supramolecules. *Cryst Eng Comm*, *14*(24), 8468-8484.

Renuga, S., & Muthu, S. (2014). Molecular structure, normal coordinate analysis, harmonic vibrational frequencies, NBO, HOMO–LUMO analysis and detonation properties of (S)-2-(2-oxopyrrolidin-1-yl) butanamide by density functional methods. *Spectrochimica Acta Part A: Molecular and Biomolecular Spectroscopy*, *118*, 702-715.

Riley, K. E., Pitonák, M., Jurecka, P., & Hobza, P. (2010). Stabilization and structure calculations for noncovalent interactions in extended molecular systems based on wave function and density functional theories. *Chemical Reviews*, *110*(9), 5023-5063.

Seth, S. K., Saha, I., Estarellas, C., Frontera, A., Kar, T., & Mukhopadhyay, S. (2011). Supramolecular self-assembly of M-IDA complexes involving lone-pair⋯ π interactions: crystal structures, hirshfeld surface analysis, and DFT calculations [H2IDA= iminodiacetic acid, M= Cu (II), Ni (II)]. *Crystal Growth & Design*, *11*(7), 3250-3265.

Smith, G., Wermuth, U. D., Healy, P. C., & White, J. M. (2007). 3, 5-dinitrosalicylic acid in molecular assembly. III.* Proton-transfer compounds of 3, 5-dinitrosalicylic acid with polycyclic aromatic and heteroaromatic amines, and overall series structural systematics. *Australian journal of chemistry*, *60*(4), 264-277.

Smith, G., Wermuth, U. D., Healy, P. C., & White, J. M. (2006). Molecular recognition in proton-transfer compounds of brucine with achiral substituted salicylic acid analogues. *Australian journal of chemistry*, *59*(5), 320-328.

Smith, G., Wermuth, U. D., Healy, P. C., Bott, R. C., & White, J. M. (2002). Structure-making with 3, 5-dimitrosalicylic acid. I. The proton transfer compounds of 3, 5-dinitrosalicylic acid with a series of aliphatic amines. *Australian journal of chemistry*, *55*(5), 349-356.

Smith, G., Hartono, A. W., Wermuth, U. D., Healy, P. C., White, J. M., & Rae, A. D. (2005). 5-Nitrosalicylic acid and its proton-transfer compounds with aliphatic Lewis bases. *Australian journal of chemistry*, *58*(1), 47-52.

Steiner, T. (2002). The hydrogen bond in the solid state. *Angewandte Chemie International Edition*, *41*(1), 48-76.

Yunus, U., Ahmed, S., Chahkandi, M., Bhatti, M. H., & Tahir, M. N. (2017). Synthesis and theoretical studies of non–covalent interactions within a newly synthesized chiral 1,2,4-triazolo [3,4-b][1, 3, 4] thiadiazine. *Journal of Molecular Structure*, *1130*, 688-698.